Passive Geared Wheel-Leg Transformable Mechanism and Robot Embodiment

Conference Paper · May 2019

CITATIONS
0

READS
547

2 authors:

Kiju Lee
Texas A&M University
41 PUBLICATIONS **623** CITATIONS
SEE PROFILE

Chuanqi Zheng
Case Western Reserve University
3 PUBLICATIONS **5** CITATIONS
SEE PROFILE

WheeLeR: Wheel-Leg Reconfigurable Mechanism with Passive Gears for Mobile Robot Applications

Chuanqi Zheng and Kiju Lee

***Abstract*— This paper presents a new passive wheel-leg transformation mechanism and its embodiment in a small mobile robot. The mechanism is based on a unique geared structure, allowing the wheel to transform between two modes, i.e., wheel or leg, potentially adapting to varying ground conditions. It consists of a central gear and legs with partial gears that rotate around the central gear to open or close the legs. When fully closed, the mechanism forms a seamless circular wheel; when opened, it operates in the leg mode. The central gear actuated by the driving motor generates opening and closing motions of the legs without using an additional actuator. The number of legs, their physical size, and the gear ratio between the central gear and the partial gears on the legs are adjustable. This design is mechanically simple, customizable, and easy to fabricate. For physical demonstration and experiments, a mobile robotic platform was built and its terrainability was tested using five different sets of the transformable wheels with varying sizes and gear ratios. For each design, the performance with successful wheel-leg transformation, obstacle climbing, and locomotion capabilities was tested in different ground conditions.**

I. Introduction

Wheel-based locomotion is the simplest, yet most effective locomotion strategy on a flat and smooth ground surface. Legged locomotion, as found in most biological systems, generates more effective movements in uneven terrain, dynamically adapting to different slopes, surface conditions, and obstacles. Wheel-leg transformable mechanisms aim to take unique advantage of each of the two types of locomotion, through either active or passive transformation between the two. An "active" mechanism uses at least one actuator to trigger the transition between the two modes. On the other hand, a "passive" mechanism transforms without using an additional actuator.

This paper presents a novel passive transformable wheel mechanism, called *WheeLeR*, its robot embodiment, and its experimental evaluation (Fig. 1). This mechanism is simple and highly customizable, warranting a broad range of potential applications in mobile robots in different scales and autonomous vehicles. Without using an additional actuator, the wheel-leg transformation can be either actively determined by the wheel's driving direction or passively triggered by external factors, e.g., obstacles or rough terrain conditions, by selecting proper design parameters.

Related Work

A broad range of active designs has been developed over the past several decades. One commonly used option is to have multiple leg segments evenly arranged around a disk, which is connected to an axial shaft. By pulling and pushing the disk, the leg segments can correspondingly open and close [1], [2], [3], [4]. Another type of design is a full wheel consisting of two half-wheels, which can be actuated to transform into legs. With a specific motor and gear arrangement, the two half-wheels can either be folded into one semicircular leg [5], [6], or deviate radially and form two legs [7]. Other than the gear transmission, wire and spring couples can also be used to generate transformation motions, e.g. *Transleg* [8]. Instead of mechanical conduction, a slip ring device can be used to transmit power and control signals, thus allowing multiple servos to fit into one single wheel and offering the wheel more degrees of freedom [9]. However, additional actuators require increased power consumption, complex mechanical design, and complicated control.

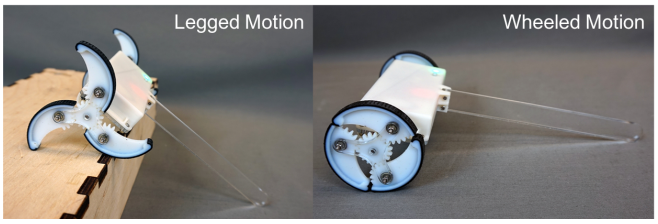

Fig. 1. A robot with transformable wheels in the leg mode for climbing an obstacle (left) and in the wheel mode on a smooth, flat surface (right).

Compared to the active mechanisms, relatively few passive mechanisms exist. One of the robots featuring a passively transformable mechanism is called *Wheel Transformer* [10], [11]. Each wheel consists of two "normal" legs, one "triggering" leg, a transmitting disc, and a spoke frame. These three legs can open passively when an external frictional force acts on the triggering leg, i.e., when encountering an obstacle. Transformation between the two modes is determined by external conditions and thus involves uncertainty. The speed in the wheel mode can also be affected when an unexpected transformation is triggered. Our design presented in this paper has a somewhat similar appearance with Wheel Transformer, however, the mechanical design, transmission type, wheel transformation mechanism, and triggering conditions are significantly different, as detailed in Section II. Another hybrid mechanism, called *Tri-Wheel*, is a three-spoke structure with a wheel installed at each end of the spoke [12]. When driven on a smooth surface, the whole structure holds its position with two of the three wheels remaining in contact with the ground. When the leading wheel encounters an obstacle, the spoke frame rolls over

Chuanqi Zheng and Kiju Lee (Corresponding Author) are with the Department of Mechanical and Aerospace Engineering at Case Western Reserve University, Cleveland, Ohio, USA. kiju.lee@case.edu

TABLE I

MAIN PARAMETERS OF LATEST TRANSFORMABLE WHEELS. *THE PRESENTED NEW DESIGN CAN HAVE A DIFFERENT NUMBER OF LEGS.

Design	Actuator	# Mode	# Legs	# Parts
Origami Wheel [2]	1	2	8	12 (5)
Passive leg [3]	1	2	5	14 (6)
T-shape leg [4]	1	2	3	9 (5)
Quattroped [5]	1	2	2	6 (6)
Turboquad [7]	1	2	2	6 (5)
Transleg [8]	1	2	1	6 (6)
Tri-wheel [12]	0	3	3	18 (7)
Wheel Trans. [10], [11]	0	2	3	6 (5)
WheeLeR	**0**	**2**	**3***	**6* (3)**

the obstacle passively while switching the contacting wheels. The driving system of this mechanism is quite complicated because it contains 14 installed gears.

Table I compares several existing transformable wheels with our new design in terms of type (i.e., active or passive), the number of modes, the number of legs when transformed, and the number of total mechanical parts (and the number of distinctive parts). The number of distinctive parts is an important design consideration because it affects the manufacturing process and cost. Since our legs are identical, increasing the number of legs does not affect the number of distinctive parts to be fabricated.

II. WHEEL-LEG TRANSFORMATION MECHANISM

This section presents the design, torque analysis, and customizable design parameters for WheeLeR, the new geared wheel-leg transformation mechanism.

A. Design Overview

The presented design is based on a geared structure shown in Fig. 2. A central gear assembles three segmented legs in place on two spoke frames, where each leg has a set of gear teeth with a mechanical lock at the end. When the central gear rotates in the clockwise (CW) direction (Fig. 2(b)), the legs open up until the central gear reaches the locks. As the central gear continues to rotate in the same direction, the entire wheel rotates in the CW direction, moving towards right in the legged motion. When the central gear rotates in the counter-clockwise (CCW) direction, the legs close and form a seamless circular wheel. As it continues rotating in the same direction, the whole mechanism rotates in the CCW direction resulting in the wheel moving towards the left. The wheel remains closed unless the driving direction is changed.

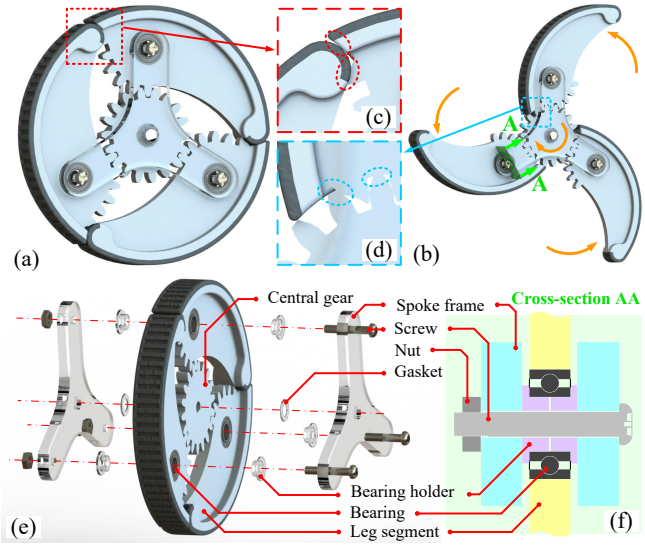

Fig. 2. CAD drawings of WheeLeR: (a) fully closed in the wheel configuration; (b) fully opened in the leg configuration; (c) mechanical lock for closed wheel; (d) mechanical lock for opened wheel; (e) assembly exploded view; and (f) AA cross-section view.

The mechanical design is simple and thus easy to fabricate. As shown in Fig. 2(e), the mechanism consists of three distinctive components: a central gear, legs, and a set of two spoke frames. For the three-leg design, only six mechanical components together with a few gaskets and screws are needed for a fully assembled structure. This is the simplest mechanism among all existing wheel-leg transformation mechanisms, as shown in Table I. In addition, this mechanism has the following unique aspects:

- The passive transformation between the two modes can be actively controlled by switching the driving direction.
- The ratio between the central gear and the partial gear (p) determines transformation tendency (Fig. 3(a,b))
- The number of legs (N_{leg}) is customizable (Fig. 3(c,d)).

B. Two Modes

The WheeLeR mechanism operates in two modes: turning in the CCW direction in the circular wheel configuration (**Mode-I**) and turning in the CW direction allowing the leg segments to open (**Mode-II**). In Mode-II, depending on the design parameters and external conditions, the mechanism may keep the legs open or dynamically switch between the wheel and leg configurations. Fig. 4 shows the torques and forces applied to the structure with the legs closed (a) and opened (b). When rotating in the CCW direction with the legs closed, the significant leg in contact with the ground is subjected to three forces: N, the reactive force from the ground to support the wheel; f, the friction force from the ground; and F_{gear}, the driving force from the central gear. The point "**A**" is the shaft around which the leg can freely

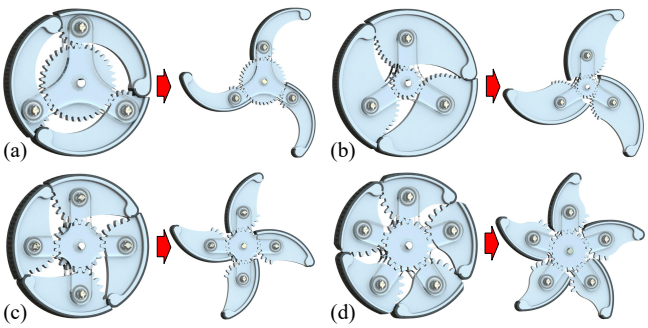

Fig. 3. Design diversification: (a) $N_{leg} = 3$ & $p = 0.5$; (b) $N_{leg} = 3$ & $p = 2$; (c) $N_{leg} = 4$ & $p = 1$; and (d) $N_{leg} = 5$ & $p = 1$.

TABLE II
NOMENCLATURE

Variable	Definition
τ_{motor}	Torque provided by motor, performed on central gear
τ_{r_f}	Torque provided by rolling friction force
τ_A	Combined torque on leg about axis A
τ_N	Torque performed about axis A, by force N
τ_f	Torque performed about axis A, by force f
τ_{gear}	Torque performed about axis A, by force F_{gear}
τ_B	Combined torque on central gear about point B
τ_C	Combined torque on opened wheel about point C
N	Reactive force from the ground to support wheel
f	Friction force from the ground (= kN)
F_{gear}	Force performed on leg through gear transmission
F_w	Robot body weight performed on central gear
k	The coefficient of rolling friction, unit in length
R	Radius of folded wheel (= $r_1 + 2r_2$)
R_{leg}	Radius of legged wheel ($\approx 2.2(r_1 + r_2)$)
r_1	Radius of central gear
r_2	Radius of partial gear on the leg
r_{sum}	Sum of r_1 and r_2 (= $r_1 + r_2$)
θ	Angle from vertical line through O towards line OA
p	Ratio of r_2 and r_1 (= r_2/r_1)

rotate. In this case, the applied torque τ_A about the axis **A** must be greater than zero, such that

$$\tau_A = F_{gear} r_2 + N L_1 + f L_2 > 0$$

where the CW direction is positive. L_1 and L_2 are the horizontal and vertical distances between **A** and the ground contact point **C**, respectively. In Mode-I, each leg makes contact with another leg at point **W**, resulting in a reactive force, F_L, such that $\tau_A = F_{gear} r_2 + N L_1 + f L_2 - F_L = 0$.

When the legs are fully open while the central gear rotates in the CW direction (Fig. 4(b)), τ_A is represented as:

$$\tau_A = -F_{gear} r_2 - N L_1 - f L_2 < 0$$

The negative value of τ_A results in the leg unfolding. A mechanical lock at the end of the gear on the leg keeps the leg in a fully opened position, resulting in $\tau_A = -F_{gear} r_2 - N L_1 - f L_2 + F'_L = 0$.

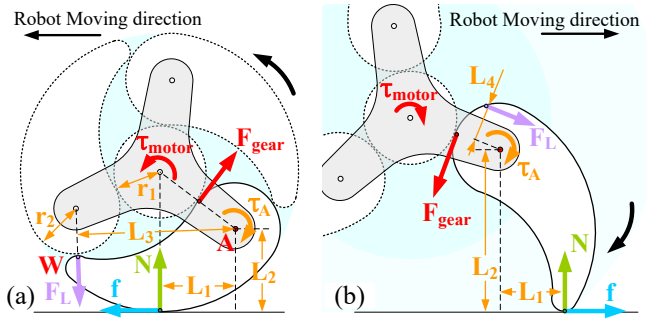

Fig. 4. Free body diagram of the wheel in two configurations: (a) circular wheel configuration in Mode-I, rotating in the CCW direction; and (b) leg configuration in Mode-II.

During the transition from the wheel to legs in Mode-II, the combined torque for the significant leg is given by (Fig. 5)

$$\tau_A = -F_{gear} r_2 + N L_1 - f L_2 \quad (1)$$

Assuming that there is no slip during rolling or transition, the effect of the rolling friction is given by

$$\tau_{r-f} = kN; \quad f = \frac{kN}{r_1 + 2r_2}$$

As shown in Fig. 5, if the robot moves towards the right in a constant speed, the torque provided by the motor, i.e., τ_{motor}, must be equal to τ_{r-f}. Then, the gear transmission force F_{gear} can be represented as:

$$F_{gear} = \frac{\tau_{motor}}{r_1} = \frac{\tau_{r-f}}{r_1} = \frac{kN}{r_1} \quad (2)$$

Also, L_1 and L_2 can be expressed as

$$L_1 = (r_1 + r_2)\sin\theta; \quad L_2 = r_1 + 2r_2 - (r_1 + r_2)\cos\theta$$

By substituting the above expressions, (1) can be rewritten as

$$\tau_A = N(r_1 + r_2)\sin\theta - kN\left(1 - \frac{(r_1 + r_2)\cos\theta}{r_1 + 2r_2} + \frac{r_2}{r_1}\right)$$

By letting $r_{sum} = r_1 + r_2$ and $p = r_2/r_1$, the above equation can be rewritten as

$$\tau_A = N \cdot \phi(k, p, r_{sum}, \theta) \quad (3)$$

where

$$\phi(k, p, r_{sum}, \theta) = r_{sum} \cdot \sin\theta - \left(p + 1 - \frac{(1+p)\cos\theta}{2p+1}\right) k.$$

C. Design Parameter Analysis

As shown in (3), τ_A is positively proportional to ϕ which is a function of k, p, r_{sum} and θ. Since θ is a variable and k cannot be customized, the analysis focuses on evaluating the effect of p and r_{sum} on the torque requirement. Given N, a higher value of ϕ indicates a higher torque, τ_A, required to trigger the wheel-leg transition. Therefore, the lower the value of ϕ the easier transition is from the wheel to the leg configuration. It is also noted that as k increases, ϕ decreases. To increase (or decrease) k, a material with a desired property may be used along the contact surfaces of the wheel.

Fig. 6 shows the relationship between $\phi(k, p, r_{sum}, \theta)$ and θ [radian] for varying $p = 0.5, 1$, and 2 and $r_{sum} = 0.015, 0.02$, and 0.025m, for $k = 0.006$. The figure shows an incremental relationship between θ and ϕ. The result

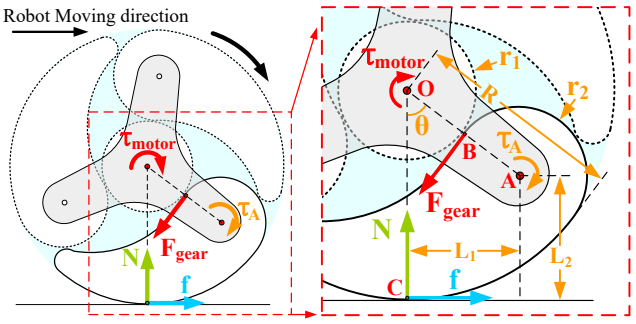

Fig. 5. Free body diagram of a closed wheel driven in the CW direction.

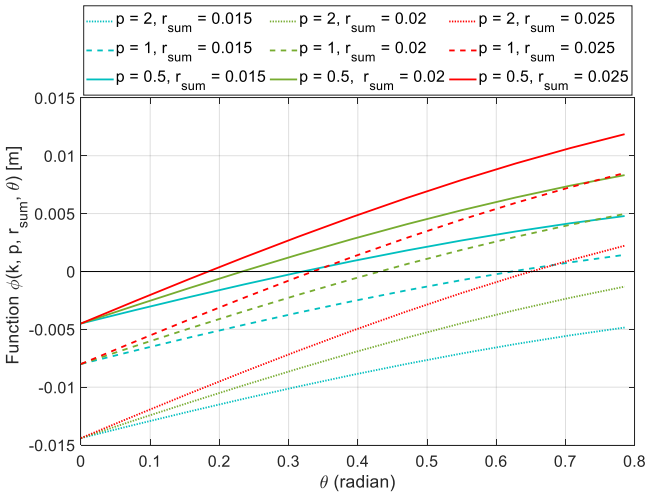

Fig. 6. $\phi(k, p, r_{sum}, \theta)$ vs. θ with $k = 0.006$.

indicates that the wheel-leg transition becomes easier when the gear side of the leg touches the ground. By comparing solid, dashed and dotted lines, it is observed that p has a significant influence on ϕ. The trends indicate that the wheels with $p = 2$ can be more easily triggered to open the legs than wheels with $p = 1$ or $p = 0.5$. In addition, r_{sum} shows a positive relation with ϕ, which means that reducing the overall wheel size can ease the triggering process. However, this negatively affects the wheel's performance on climbing over an obstacle or moving on a rough terrain.

D. Minimum Motor Torque Requirement

Analysis of the minimum motor torque requirement focused on estimating the torque required for successful wheel-leg transformation as well as climbing over an obstacle. Fig. 7(a) shows the central gear during the transition. The required torque to rotate the central gear in the CW direction is:

$$\tau_{actual} = \tau_{motor} - F_w L_5 = \tau_{motor} - F_w r_1 \sin\alpha > 0 \quad (4)$$

The motor torque requirement reaches the maximum when $\alpha = \pi/2$. Substituting $r_1 = 1.3$(cm), $F_w = 0.6$(N), and $\alpha = \pi/2$ to (4), we have

$$\tau_{motor} > F_w r_1 \sin\alpha = 0.081 \text{ [kg} \cdot \text{cm]} \quad (5)$$

Fig. 7(b) shows an opened wheel climbing onto a flat platform. Without any relative motion between the gears, the wheel is taken as one piece in this scenario. The required torque to rotate the wheel in the CW direction is:

$$\tau_C = \tau_{motor} - F_w L_6 = \tau_{motor} - F_w(R_{leg}) \sin\beta > 0 \quad (6)$$

Similarly, the requirement of motor torque reaches maximum when $\beta = \pi/2$. Substitute $R_{leg} = 2.2(r_1 + r_2)$ (can be easily calculated by wheel geometric structure), $r_1 + r_2 = 2.5$, $F_w = 0.6$ and $\beta = \pi/2$ to (6), we have:

$$\tau_{motor} > 2.2 F_w (r_1 + r_2) \sin\beta = 0.337 \quad (7)$$

By comparing (5) and (7), the minimum motor torque requirement is obtained: $\tau_{motor} > 0.337$.

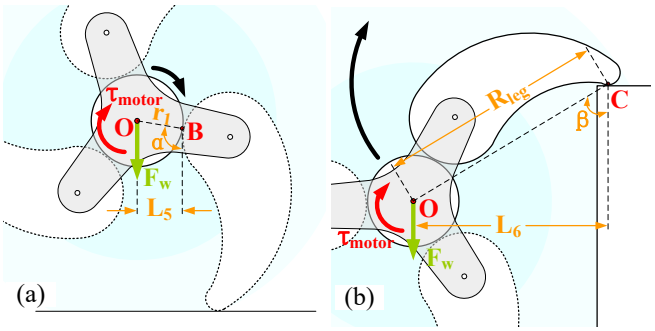

Fig. 7. (a) Free body diagram of central gear during transformation process; and (b) climbing onto an obstacle with the legs open.

III. Robot Embodiment and Experiments

For technical feasibility and locomotion capability evaluation, a mobile robot with two WheeLeR mechanisms was designed and built, as shown in Fig. 8.

A. Hardware Design

A fully assembled robot consists of a main body chassis, a tail, and two transformable wheels (Fig. 8(a)). The overall dimensions of the robot are shown in Fig. 8(b). The chassis is a cuboid box made of an acrylic base and a 3D-printed ABS shell. Two gear motors were installed beneath the base, with the motor shafts laterally extruded. As the robot is expected to move on a rough terrain, a bumper at the front bottom of the base was attached to protect the motors and gears from external impacts. The tail is an acrylic bar, to support the robot when climbing an obstacle. The tail has a smooth curved tip, in order not to interfere with the robot's locomotion in either direction. Three different lengths for the tail (i.e., 90, 120, and 150mm) were fabricated for testing the robot in different terrain conditions and at different obstacle heights. For the transformable wheels, the spoke frames were made of acrylic, while the gears and legs are 3D printed by a Polyjet 3D printer Object350 Connex3. Each leg was printed using two different materials, a rigid material (i.e., VeroWhite) for the main leg structure and a soft material (i.e., AgilusBlack) along the outer surface to increase friction between the leg and the ground.

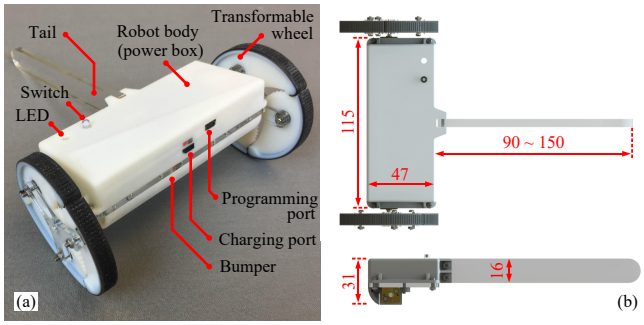

Fig. 8. A mobile robot with two transformable wheels: (a) fully assembled robot; and (b) its overall dimensions in millimeters (mm).

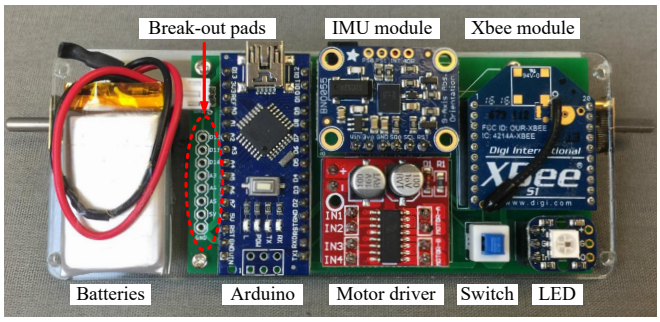

Fig. 9. Embedded electronic components.

Fig. 9 shows the embedded electronic components: two 3.7V Lithium-polymer batteries, an XBee module for wireless communication and remote control, an Arduino Nano as the main processing board, a Neo-pixel LED for status indication, and a motor driver. All electronic components were mounted on the top of the main chassis. Two N20 gear motors were used to actuate two wheels individually. The motor shaft was directly connected to the central gear of the wheel. Based on (7), we selected the gear ratio of 150:1 for the motors to provide a rated torque of 0.4kg·cm. The robot was also equipped with an Inertial Measurement Unit (IMU), consisting of tri-axial accelerometer and tri-axial gyroscope. The IMU can be used to determine the transformation between the two modes. For example, if the robot encounters a rough surface or gets stuck, as detected by the IMU while moving on the wheel mode, it turns around and proceeds with the leg mode. The embedded printed circuit board was built with break-out pads for extension. Different types of application-specific sensors can be added.

B. Experiments

To test wheel transformation conditions and robot locomotion capability, a series of experiments were conducted. The transformation success rate on different terrains, the maximum obstacle height for different radii of the wheel, and the speed of the robot in each mode were measured.

1) Transformation tendency: While the driving direction determines the mode (i.e., Mode-I or Mode-II), WheeLeR's behavior in Mode-II differs depending on the design parameters and environmental conditions. In other words, with a low transformation tendency, the wheels may remain closed until it encounters an obstacle, while with a high transformation tendency, they would immediately transform into legs even on a smooth, flat surface. The first case would be useful when the surface conditions are unknown and dynamically changing while the triggering behavior would involve higher uncertainty. The latter case would be more suitable when precise control between the two modes is desired. In such a situation, the robot's driving direction determines the mode of the wheels and triggers the transformation.

To evaluate the wheel-leg transition tendency, five sets of wheels with different pairs of r_{sum} and p values were built and tested on eight terrain types, as shown in Fig. 10. For each combination, the experiment was conducted five times, each containing twenty trials. To test the effect of the wheel size, three different values of $r_{sum} = 25/20/15$mm (i.e., $R = 37.5/30/22.5$) were considered while keeping $p = 1$. The results showed that the wheel size has no significant effect on the transformation success rate. On the other hand, the success rate was highly correlated with p. Comparing the three sets of wheels with $p = 0.5, 1,$ and 2 ($r_{sum} = 20$), the wheels with $p = 0.5$ showed the lowest transformation success rate, while ones with $p = 2$ could successfully transform in most of the selected terrain types. These experimental results are also consistent with the numerical analysis shown in Fig. 6.

Fig. 11 and Fig. 12 show different behaviors of the wheels with two different values of p. Fig. 11 shows the robot using the wheels with $r_{sum} = 20$ and $p = 2$ climbing over a 90mm obstacle. Since these wheels have a very high transformation tendency, the wheels transform immediately after the robot changes the driving direction even before reaching the obstacle. However, with $p = 1$, the wheels remain closed until reaching the obstacle, as shown in Fig. 12. In this situation, the obstacle exerts extra friction to the wheel and triggers the transformation.

2) Obstacle climbing capability: Three sets of wheels ($R = 37.5/30/22.5$mm with $p = 1$ and $N_{leg} = 3$) were chosen to test the ability to climb obstacles with different heights. For each height, a success rate was calculated from 50 trials. The experimental result in Table III shows that the robot is able to climb over an obstacle that is up to 2.4 times the height of the wheel radius (R). For an obstacle higher than about 2.67 times of the wheel diameter, about 50% of the success rate was observed. Table III shows how to determine the wheel size for expected heights of obstacles.

3) Locomotion speed: Three sets of wheels ($R = 37.5/30/22.5$mm with $p = 1$ and $N_{leg} = 3$) were again used to estimate robot locomotion speed in two modes. On a flat asphalt surface in the wheel mode, the speed was measured at 0.30, 0.26 and 0.19m/sec, respectively. In this case, the speed was approximately proportional to R. When driven on the same surface with the legs open, the speed was measured at 0.24, 0.25 and 0.21m/sec, respectively. Walking with the largest wheels ($R = 37.5$) with the legs open required high torque, resulting in the motor operating in a slower speed than the rated value. This caused the line speed to be even slower than that using wheels with a smaller radius $R = 30$. To resolve this, the motor gear ratio can be increased or more powerful motors can be used.

IV. Conclusion and Future Work

We presented a new passive wheel-leg transformable mechanism, called WheeLeR. This mechanism allows the wheel to operate in two modes, in order to adapt to both flat and rough terrains. It is based on a simple geared structure, consisting of a central gear, legs, and a set of two spoke frames. While only the three-leg designs were used for design validation and experiments, WheeLeR is highly customizable in terms of R, N_{leg}, and p. Depending

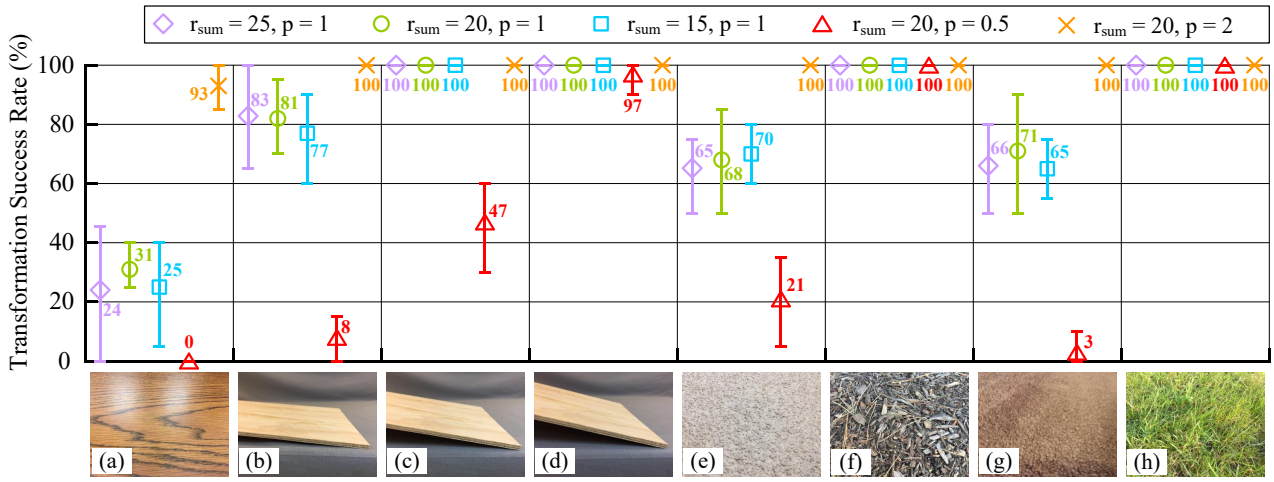

Fig. 10. Plots of wheel transformation success rate versus different wheel designs and terrain types: (a) flat surface; (b) 5 degree slope; (c) 10 degree slope; (d) 15 degree slope; (e) asphalt (3mm rigid); (f) rugged surface (10mm rigid); (g) carpet (8mm flexible); (h) grass (80mm flexible)

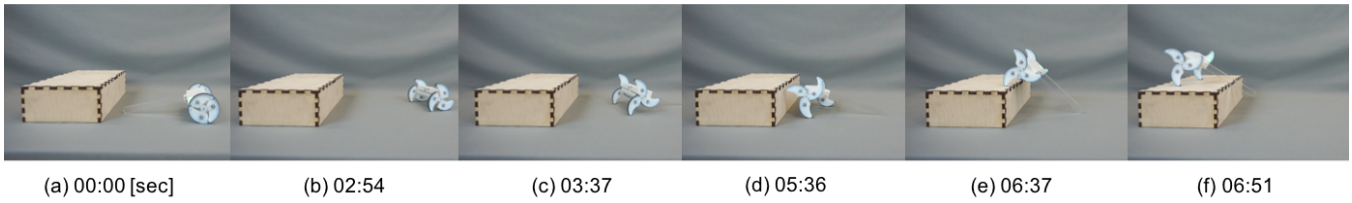

Fig. 11. Process of climbing 90mm obstacle using wheels with $r_{sum} = 20$ and $p = 2$: The robot in Mode-I encounters obstacle (a); turns around to switch to Mode-II, immediately opening the legs (b); approaches the obstacle (c); and climbs over the obstacle (d-f).

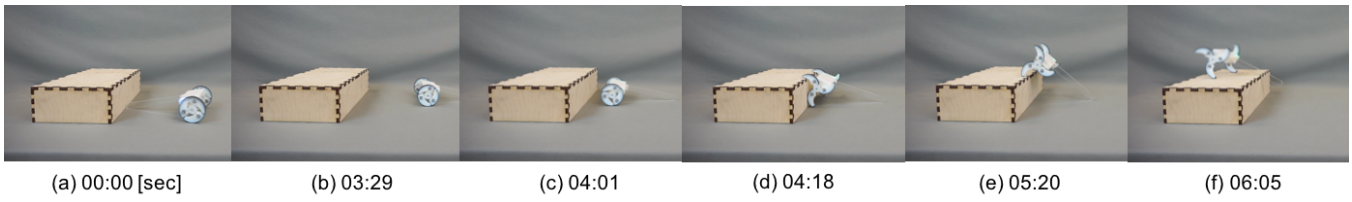

Fig. 12. Process of climbing 90mm obstacle using wheels with $r_{sum} = 20$ and $p = 1$: The robot in Mode-I encounters obstacle (a); turns around to switch to Mode-II, but legs remain closed (b-c) until it hits the obstacle and triggers opening the legs (d); and climbs over the obstacle (e-f).

TABLE III
SUCCESS RATE (%) OF CLIMBING AN OBSTACLE.

Obstacle height (mm)	$R = 37.5$	$R = 30$	$R = 22.5$
30	100	100	100
40	100	100	100
50	100	100	90
60	100	100	48
70	100	96	-
80	100	68	-
90	82	-	-
100	56	-	-

on the types and sizes of the obstacles and ground surface types/conditions, these design parameters can be carefully selected to achieve effective locomotion.

Parameter analysis was conducted on wheel-leg transition triggering conditions and minimum motor torque requirements. The result indicates that the triggering process is more likely to be initiated at position $\theta = 0$. Besides, increasing p or decreasing r_{sum} may result in a higher transformation tendency. For physical demonstration and evaluation, a robot together with five sets of wheels were built. The experimental results confirmed that a higher p value has a higher transformation success rate, while r_{sum} showed only trivial effect. Obstacle climbing tests indicated that the wheels can easily climb over obstacles that are up to 2.4 times the height of the wheel radius. With appropriate wheel configuration, the speed could reach 0.30m/sec with wheels and 0.25 with legs.

For a fully autonomous performance, additional sensors, such as a camera, may be added to the robot for navigation in an unknown environment. Using the embedded IMU integrated with the camera inputs, the robot may autonomously change its mode to effectively adapt its wheel configuration to the environmental conditions.

REFERENCES

[1] K. Nagatani, M. Kuze, and K. Yoshida, "Development of transformable mobile robot with mechanism of variable wheel diameter," *J. Robot. Mechatron*, vol. 19, pp. 252–253, 2007.

[2] D.-Y. Lee, S.-R. Kim, J.-S. Kim, J.-J. Park, and K.-J. Cho, "Origami wheel transformer: A variable-diameter wheel drive robot using an origami structure," *Soft robotics*, vol. 4, no. 2, pp. 163–180, 2017.

[3] Y. She, C. J. Hurd, and H.-J. Su, "A transformable wheel robot with a passive leg," in *Intelligent Robots and Systems (IROS), 2015 IEEE/RSJ International Conference on*. IEEE, 2015, pp. 4165–4170.

[4] T. Sun, X. Xiang, W. Su, H. Wu, and Y. Song, "A transformable wheel-legged mobile robot: Design, analysis and experiment," *Robotics and Autonomous Systems*, vol. 98, pp. 30–41, 2017.

[5] S.-C. Chen, K.-J. Huang, W.-H. Chen, S.-Y. Shen, C.-H. Li, and P.-C. Lin, "Quattroped: a leg–wheel transformable robot," *IEEE/ASME Transactions On Mechatronics*, vol. 19, no. 2, pp. 730–742, 2014.

[6] M. Ning, B. Xue, Z. Ma, C. Zhu, Z. Liu, C. Zhang, Y. Wang, and Q. Zhang, "Design, analysis, and experiment for rescue robot with wheel-legged structure," *Mathematical Problems in Engineering*, vol. 2017, 2017.

[7] W.-H. Chen, H.-S. Lin, Y.-M. Lin, and P.-C. Lin, "Turboquad: a novel leg–wheel transformable robot with smooth and fast behavioral transitions," *IEEE Transactions on Robotics*, vol. 33, no. 5, pp. 1025–1040, 2017.

[8] Z. Wei, G. Song, Y. Zhang, H. Sun, and G. Qiao, "Transleg: A wire-driven leg-wheel robot with a compliant spine," in *Information and Automation (ICIA), 2016 IEEE International Conference on*. IEEE, 2016, pp. 7–12.

[9] K. Tadakuma, R. Tadakuma, A. Maruyama, E. Rohmer, K. Nagatani, K. Yoshida, A. Ming, M. Shimojo, M. Higashimori, and M. Kaneko, "Mechanical design of the wheel-leg hybrid mobile robot to realize a large wheel diameter," in *Intelligent Robots and Systems (IROS), 2010 IEEE/RSJ International Conference on*. IEEE, 2010, pp. 3358–3365.

[10] Y.-S. Kim, G.-P. Jung, H. Kim, K.-J. Cho, and C.-N. Chu, "Wheel transformer: A miniaturized terrain adaptive robot with passively transformed wheels," in *Robotics and Automation (ICRA), 2013 IEEE International Conference on*. IEEE, 2013, pp. 5625–5630.

[11] Y.-S. Kim, G.-P. Jung, H. Kim, K.-J. Cho, and C. N. Chu, "Wheel transformer: A wheel-leg hybrid robot with passive transformable wheels," *IEEE Transactions on Robotics*, vol. 30, no. 6, pp. 1487–1498, 2014.

[12] L. M. Smith, R. D. Quinn, K. A. Johnson, and W. R. Tuck, "The tri-wheel: A novel wheel-leg mobility concept," in *Intelligent Robots and Systems (IROS), 2015 IEEE/RSJ International Conference on*. IEEE, 2015, pp. 4146–4152.